is not hydrolyzed by treatment with strong acids (Table 1). Hydrolysis-resistant amides have been observed in marine particulate matter and sediments, where the resistance to chemical hydrolysis has been attributed to physical sorption and encapsulation (*30*). Amide-N in DON is not physically protected, but previous experiments have shown that the biodegradation rate of labile compounds such as proteins is substantially reduced by abiotic complexation within marine DOM (*31*). Long-term protein-DOM interactions may lead to structural modifications that render proteins resistant to chemical hydrolysis and unavailable to bacteria. This mechanism could lead to the sequestration of nitrogen in the dissolved phase (*32*) and give rise to the hydrolysis-resistant amide-N observed by ^{15}N-NMR.

Our data show that two chemically distinct pools of organic nitrogen accumulate in the ocean. The higher concentration of HMWDON in the mixed layer (relative to deep ocean values) largely reflects the presence of *N*-AAPs, which degrade on time scales of upper ocean mixing. These newly added biopolymers are chemically distinct from the refractory HMWDON pool that exists throughout the water column. If we assume the proportion of *N*-AAPs, protein, and nonhydrolyzable amide measured in our samples is representative of global HMWDON, then as much as 80% of the decrease in HMWDON with depth involves the removal of *N*-AAPs. The abundance of amide-N throughout the water column suggests amides are more biologically recalcitrant than other forms of organic-N. The ubiquity of amide linkages in HMWDON is not surprising, given that most organic nitrogen in phytoplankton is protein. However, the important contribution of *N*-AAPs to upper ocean HMWDOM, and the resistance of amides in deep sea HMWDOM to chemical and biological degradation, are unexpected results that help elucidate the currency of DON in the marine nitrogen cycle.

References and Notes

1. J. Abell, S. Emerson, P. Renaud, *J. Mar. Res.* **58**, 203 (2000).
2. M. J. Church, H. W. Ducklow, D. M. Karl, *Limnol. Oceanogr.* **47**, 1 (2002).
3. P. Libby, P. Wheeler, *Deep-Sea Res.* **44**, 345 (1997).
4. N. J. Antia, P. J. Harrison, L. Oliveira, *Phycologia* **30**, 1 (1991).
5. T. Berman, D. A. Bronk, *Aquat. Microb. Ecol.* **31**, 279 (2003).
6. D. A. Bronk, in *Biogeochemistry of Marine Dissolved Organic Matter*, D. A. Hansell, C. A. Carlson, Eds. (Academic Press, San Diego, CA, 2002), pp. 163–247.
7. HMWDON is defined here as the fraction of DON retained by an ultrafiltration membrane with a pore size of 1 nm. This fraction is expected to have a nominal molecular weight of >1 kD.
8. M. D. McCarthy, T. Pratum, J. I. Hedges, R. A. Benner, *Nature* **390**, 150 (1997).
9. M. D. McCarthy, J. I. Hedges, R. A. Benner, *Science* **281**, 231 (1998).
10. L. I. Aluwihare, D. J. Repeta, R. F. Chen, *Deep-Sea Res. II* **49**, 4421 (2002).
11. L. I. Aluwihare, D. J. Repeta, R. F. Chen, *Nature* **387**, 166 (1997).
12. S. Henrichs, P. M. Williams, *Mar. Chem.* **17**, 141 (1985).
13. De-acetylation of HMWDON samples was performed in 1 N HCl. Samples were heated overnight at 90°C under an atmosphere of N_2. The acetic acid produced during the hydrolysis was extracted from a weighed aliquot of the hydrolysate into either ethyl ether or dichloromethane. After extraction, the presence of acetic acid in the organic fraction was confirmed by solution-state ^{1}H-NMR before low molecular weight acids (e.g., acetic acid) were quantified. The aqueous fraction of the hydrolysate was lyophilized and, as shown in the ^{1}H-NMR (Fig. 2C), no longer contained acetamide. Changes in C and N were assessed with solid-state ^{13}C- and ^{15}N-NMR spectroscopy. Under these hydrolysis conditions, no muramic acid (de-acetylated) or amino sugar monomers were detected.
14. D. B. Albert, C. S. Martens, *Mar. Chem.* **56**, 27 (1997).
15. M. Zhao, J. L. Bada, *J. Chromatogr. A.* **690**, 55 (1995).
16. The percentage of N in each sample represented by *N*-AAPs, hydrolyzable protein, and nonhydrolyzable amide was calculated as follows: Because 1 mol of *N*-AAP sugar is de-acetylated for every mole of acetic acid released, we assumed that μmoles of acetic acid were equal to μmoles of N in *N*-AAPs; hydrolyzable protein N was calculated on the basis of the recoveries of amino acid N after strong acid hydrolysis (*12*); nonhydrolyzable amide was determined after strong acid hydrolysis (Table 1). Higher amino acid yields were obtained when HMWDON was hydrolyzed with strong acid. As a result, after strong acid hydrolysis, only 2.2 (29% of total N) and 5.5 μmol (71% of total N) of amide-N remained unhydrolyzed in the Woods Hole and MAB samples, respectively. In order to quantify the amount of amide-N remaining after strong acid hydrolysis, the sum Σacetic acid (mild) + amino acids (strong) was first determined and then subtracted from the initial amide content of the HMWDON sample (before hydrolysis). In all cases, percentages are expressed relative to total N in each sample. We calculated the amount of *N*-AAP carbon with the C/N ratio in HMWDOM (Table 1) and assumed 8 μmol of C per μmol of *N*-AAP (e.g., *N*-acetyl glucosamine).
17. J. J. Boon, V. A. Klap, T. I. Eglinton, *Org. Geochem.* **29**, 1051 (1998).
18. J. A. Leenheer, T. I. Noyes, C. E. Rostad, M. L. Davisson, *Biogeochemistry* **69**, 125 (2004).
19. K. Kaiser, R. Benner, *Anal. Chem.* **72**, 2566 (2000).
20. D. L. Popham, J. Helin, C. E. Costello, P. Setlow, *J. Bacteriol.* **178**, 6451 (1996).
21. We modified the method provided in (*20*) and hydrolyzed samples (in 4 N HCl) overnight at 90°C. We recovered no muramic acid and only small amounts of glucosamine and galactosamine from surface samples. This modified hydrolysis method was tested on chitin oligomers, peptidoglycan (from *Bacillus subtilus*), and bacterial cells (mixed laboratory culture) to ensure the quantitative (>90%) recovery of glucosamine and de-acetylated muramic acid. We assessed amino sugar recoveries by high-performance liquid chromatography and fluorescence detection of *o*-phthaldialdehyde-derivatized samples (*15*) or gas chromatography after derivatizing to alditol acetates (*10*).
22. J. I. Hedges *et al.*, *Org. Geochem.* **31**, 945 (2000).
23. O. Hadja, *Anal. Biochem.* **60**, 512 (1974).
24. Y. Nagata, T. Fujiwara, K. Kawaguchinagata, Y. Fukumori, T. Yamanaka, *Biochim. Biophys. Acta* **1379**, 76 (1998).
25. J. S. Martinez *et al.*, *Science* **287**, 1245 (2000).
26. B. Palenik, S. E. Henson, *Limnol. Oceanogr.* **42**, 1544 (1997).
27. M. T. Cottrell, D. L. Kirchman, *Appl. Environ. Microbiol.* **66**, 1692 (2000).
28. A. L. Svitil, D. L. Kirchman, *Microbiol.* **144**, 1299 (1998).
29. M. T. Cottrell, D. N. Wood, L. Yu, D. L. Kirchman, *Appl. Environ. Microbiol.* **66**, 1195 (2000).
30. H. Knicker, P. G. Hatcher, *Naturwissenschaften* **84**, 231 (1997).
31. R. G. Keil, D. L. Kirchman, *Mar. Chem.* **45**, 187 (1994).
32. E. Tanoue, S. Nishiyana, M. Kamo, A. Tsugita, *Geochim. Cosmochim. Acta* **59**, 2643 (1995).

33. We thank A. Beilecki, then at Brüker Instruments, for assistance with ^{15}N-NMR spectroscopy; M. Pullin and D. Albert for assistance in the determination of acetic acid; and the staff at the Natural Energy Laboratory in Kona, Hawaii, and E. Smith for assistance in sample collection. Supported by the Chemical and Biological Oceanography Programs at the National Science Foundation; the Carbon Sequestration Program at the U.S. Department of Energy; the Rhinehart Coastal Research Center of the Woods Hole Oceanographic Institution; and the Fundación Andes, Chile.

20 December 2004; accepted 9 March 2005
10.1126/science.1108925

Assessing Methane Emissions from Global Space-Borne Observations

C. Frankenberg,[1] J. F. Meirink,[2] M. van Weele,[2] U. Platt,[1] T. Wagner[1]

In the past two centuries, atmospheric methane has more than doubled and now constitutes 20% of the anthropogenic climate forcing by greenhouse gases. Yet its sources are not well quantified, introducing uncertainties in its global budget. We retrieved the global methane distribution by using space-borne near-infrared absorption spectroscopy. In addition to the expected latitudinal gradient, we detected large-scale patterns of anthropogenic and natural methane emissions. Furthermore, we observed unexpectedly high methane concentrations over tropical rainforests, revealing that emission inventories considerably underestimated methane sources in these regions during the time period of investigation (August through November 2003).

Methane (CH_4) is, after carbon dioxide (CO_2), the second most important anthropogenic greenhouse gas (*1*). It also has an indirect effect on climate through chemical feedbacks (*1*, *2*). More than 50% of present-day global methane emissions are anthropogenic, the largest contributors being fossil fuel production, ruminants, rice cultivation, and waste handling (*3*). The natural source strength of CH_4, mainly constituted by wetlands, is particularly uncertain, because these emissions vary considerably in time and space (*4*, *5*) and available ground-based measurements are sparse, albeit precise, and limitedly representative at larger scales. Better knowl-

[1]Institute of Environmental Physics, University of Heidelberg, INF 229, 69120 Heidelberg, Germany. [2]Section of Atmospheric Composition, Royal Netherlands Meteorological Institute, Post Office Box 201, 3730 AE De Bilt, Netherlands.

edge of the methane distribution and emissions is indispensable for a correct assessment of its impact on global change (*1*). Observations from space now allow the global detection of spatial and temporal variations in atmospheric methane concentrations, thereby enabling identification of known sources and discovery of new ones, particularly in regions that are poorly sampled by existing surface measurement networks.

The SCIAMACHY (scanning imaging absorption spectrometer for atmospheric chartography) instrument (*6*) on board the European Space Agency (ESA)'s environmental research satellite ENVISAT records the intensity of solar radiation, reflected from the Earth surface or the atmosphere, in more than 8000 spectral channels between 240 and 2390 nm. From these measurements, atmospheric trace gas concentrations (e.g., BrO, OClO, H_2O, SO_2, NO_2, CH_2O, O_3, N_2O, CO, CH_4, and CO_2) can be derived (*7*, *8*). The near-infrared spectrometers are used for global measurement of total columns of carbon monoxide and greenhouse gases carbon dioxide and methane. ENVISAT operates in a nearly polar, sun-synchronous orbit at an altitude of 800 km, crossing the equator at 10:00 a.m. local time. SCIAMACHY offers a variety of measurement geometries. For column retrievals, we chose the nadir mode in which the instrument points down almost perpendicular to the earth's surface, detecting reflected sunlight. The spatial extent of the ground pixels considered in this study is 60 km (east-west) by 30 km (north-south). Global coverage is achieved every 6 days.

CO_2 and CH_4 not only absorb thermal radiation from the Earth system, causing radiative forcing, but also solar radiation in the near-infrared. Hence, these molecules can be measured by means of the proven method of differential optical absorption spectroscopy (*9*) (DOAS). To account for peculiarities of spectrometry in the near-infrared (*10*, *11*), we implemented a new modified iterative algorithm (IMAP-DOAS) (*12*) that enables precise and unbiased determination of vertical column densities (VCDs, the vertically integrated concentrations from surface to top of atmosphere) of methane and carbon dioxide. The negligibility of Rayleigh scattering proves to be a major advantage in the near-infrared: In the absence of clouds and aerosols, most photons recorded by the instrument have thus been reflected at the Earth's surface, thereby having traversed the entire atmospheric column twice. This renders the measurements sensitive to the lower troposphere, which is a prerequisite for the detection of near-ground methane sources. In contrast, thermal-infrared sounders, which have also been used to measure CH_4 (*13*), exhibit a lack of sensitivity near the ground. However, they could derive methane abundances in the free troposphere and stratosphere, thus yielding more accurate information about the lower troposphere when synergistically combined with near-infrared retrievals.

Two main points affecting the retrieval in the near-infrared have to be considered: First, the VCD of a well-mixed gas scales linearly with the total column of all atmospheric constituents, thus with surface pressure. Hence, we need a proxy for surface pressure to convert columns into mixing ratios. Second, clouds and aerosols can substantially alter the light path of the recorded photons. CO_2 exhibits only very small variations in its total columns, and the retrieval window (1562 to 1585 nm) is spectrally close to the CH_4 retrieval window (1630 to 1670 nm). Thus, it is well suited as a proxy for both surface pressure (or, in the presence of clouds, cloud top pressure) and changes in the light path due to partial cloud cover and aerosols. Consequently, we can derive the column-averaged dry (no water vapor included) volume mixing ratio (VMR) of CH_4 in the atmosphere from the ratio of the CH_4 VCD (V_{CH_4}) and the CO_2 VCD (V_{CO_2}), scaled by the global and annual mean of the CO_2 column-averaged mixing ratio [370 parts per million (ppm)], i.e., $VMR(CH_4) \approx V_{CH_4}/V_{CO_2} \cdot \overline{VMR}(CO_2)$. Care should be taken not to confuse column-averaged VMRs with surface VMRs. Surface VMRs have a stronger response to emissions, whereas column-averaged mixing ratios exhibit less variation and are slightly lower because of reduced methane VMRs in the stratosphere.

A retrieval bias is introduced by assuming a constant column-averaged VMR(CO_2), whereas in reality it varies globally and seasonally over a range (minimum to maximum) of about 11 ppm by volume or 3% (*14*). This bias will be largest in Eurasia and North America north of 40°N. However, south of 40°N the bias can be assumed to be within 1.5% (*14*). Methane enhancements may be masked by our method in cases of sources leading to similar relative enhancements of V_{CO_2} and V_{CH_4} (e.g., biomass burning for certain fire types).

In the next step, we discard all measurements exhibiting substantial cloud cover at altitudes substantially above the ground, because we are primarily interested in variations in the lower troposphere. Figure 1A demonstrates how we extracted appropriate measurements: Highest CO_2 column observations show strong anticorrelation with surface altitude, illustrating the sensitivity to the boundary layer and being a first proof of the quality of the measurements. Strongly reduced column retrievals can be attributed to the shielding effect of clouds. We used a lower threshold of V_{CO_2} (red line) to obtain a suitable subset of measurements (gray pixels) representing the lower troposphere. A scatter plot of V_{CO_2} and V_{CH_4} underlines the close correlation of both measurements in this subset (Fig. 1A). The deviations from the strictly linear correlation bear the actual information, i.e., the variations of the CH_4 column with respect to the CO_2 column, which is determined by the length of the light path and an only slightly varying CO_2 VMR.

By using only the aforementioned measurement subset, we averaged the CH_4 VMRs from August through November 2003 on a horizontal grid (1° by 1°) as shown in Fig. 2. The latitudinal gradient in the methane VMRs can be seen, with strongest gradients, as expected, across the Intertropical Convergence Zone (ITCZ). Apart from this gradient, large-scale and strong methane enhancements are observed in various parts of the world. The largest abundances are found in the Gangetic plains of India, Southeast Asia, and parts of China. According to current emission inventories (fig. S1) (*3*), the sources can be mostly attributed

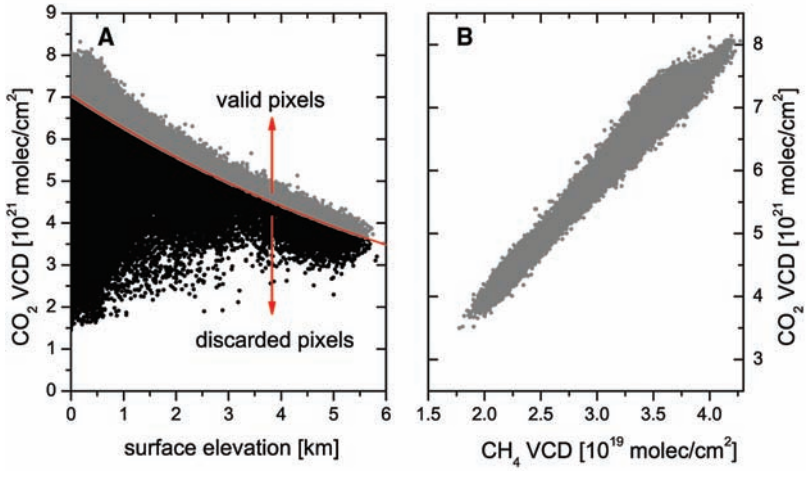

Fig. 1. (**A**) A scatter plot of the retrieved CO_2 VCDs versus surface altitude (August to September 2003). For further evaluations, only pixels above the threshold indicated by the red line are considered (corresponding to an effective cloud top height of 1 km). (**B**) A scatter plot of the retrieved vertical column densities of CH_4 and CO_2 for all valid pixels. The slight deviations from the strictly linear correlation between both VCDs can be mostly explained by variations in the CH_4 VMRs.

to rice cultivation in this time period and, to a lesser extent, to domestic ruminants. Wetlands presumably caused the observed high abundances in central Africa and Manchuria in China. Fossil fuel production can be associated with enhanced CH_4 VMRs over the industrialized Yellow river basin in China and the Appalachian basin (coal mining) in the eastern United States. Waste treatment–related emissions are likely to add to these in populated areas.

To substantiate our findings, we compared the measurements with methane concentration fields simulated with use of a global chemistry-transport model (TM3) (*15*) that takes current emission inventories (*16*, *17*) into account (fig. S1). The modeled enhancements in the United States and Asia as well as the north-south gradient (Fig. 3) strongly resemble the methane VMRs retrieved by SCIAMACHY in magnitude and spatial extent (Fig. 2). Additionally, persistent long-range transport features are observed, most clearly over the Pacific east of Japan (movie S1 and Fig. 2). In principle, the model enables discrimination of emissions and transport, e.g., evident in November 2003, with Africa strongly influenced by methane transported from South Asia (movie S1).

Although the general agreement between the measurements and the model is very good (fig. S2), there are discrepancies in India and in the tropics (Fig. 3B). The measured abundances over India are lower than that simulated by the model. This indicates that the rice emissions used in our model runs (amounting to 80 Tg $year^{-1}$) were probably overestimated. In contrast, SCIAMACHY retrievals in the tropics are up to 4% [70 parts per billion (ppb)] higher than predicted by the model.

We verified that this discrepancy cannot be attributed to a retrieval error dependent on solar zenith angle, light-path changes, or albedo [Supporting Online Material (SOM) Text]. A model bias, such as an underestimate of the stratospheric methane abundances or large errors in the modeled distribution of OH radicals, can also be excluded (SOM Text). The higher methane VMRs of the measurement compared with the model can thus be explained either by tropical methane emissions not considered in the model, a regional CO_2 depression relative to the annual global mean, or some combination of both. Although CO_2 flux estimates in the tropical land masses are uncertain (*18*), the required depression in the CO_2 column (3 to 4%) would have an improbably high magnitude (*14*). Hence, we conclude that tropical CH_4 sources in our model are underestimated.

The underestimate may be related to biogenic methane emissions, because there is a strong spatial correlation between the discrepancies and the presence of broadleaf evergreen forest (fig. S3) (*19*). Model simulations indicate that an additional tropical methane source of around 30 Tg over the considered time period (August through November) is needed if the discrepancy is fully assigned to methane sources. For comparison, the tropical source in our model is 45 Tg (table S1). Potential candidates for the enhanced source include wetlands, biomass burning, termites, cattle breeding in pastures, or a hitherto unknown methane source that might be directly related to the broadleaf evergreen forest. Wetland emissions, in particular in the Amazon, appear to be underestimated in our model [e.g., Melack *et al*. (*20*) estimate an annual source of 29 Tg of CH_4 for the Amazon, whereas we used 8 Tg], but the investigated period coincides with the dry season in most of the tropics, when wetland emissions are supposed to be lowest (*20*, *21*). However, in the dry season unaccounted biomass burning can also contribute to the discrepancy. Tropical fires are characterized by a molar CH_4/CO_2 ratio (*22*) that is more than twice the ratio of their respective background concentrations. Hence, our measurements are sensitive to these fires. Lastly, termites constitute a substantial but poorly constrained tropical methane source (*23*). Further validation measurements and process-based investigations for the considered

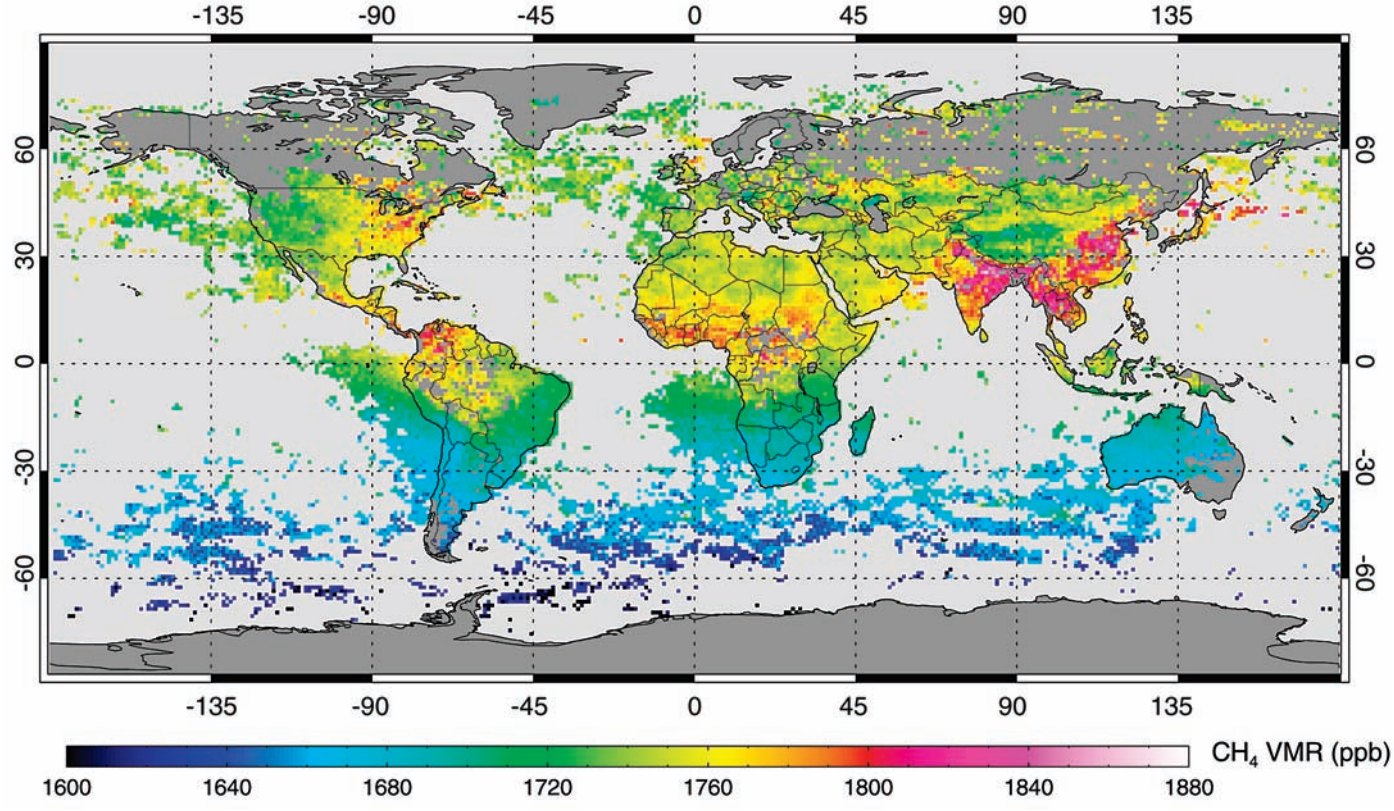

Fig. 2. SCIAMACHY measurements of column-averaged methane VMR in ppb units. The measurements are averaged over the time period of August through November 2003 on a 1° by 1° horizontal grid. At least 5 (and up to 150) measurements are taken for each grid cell. Only few observations are available over the ocean, because low ocean reflectivity substantially reduces the quality of the retrieval, leading in turn to unreliable measurements (standard deviation of the fit residual above 0.5%) that are discarded. Occasionally, sun glint or clouds at low altitudes allow measurement over the ocean.

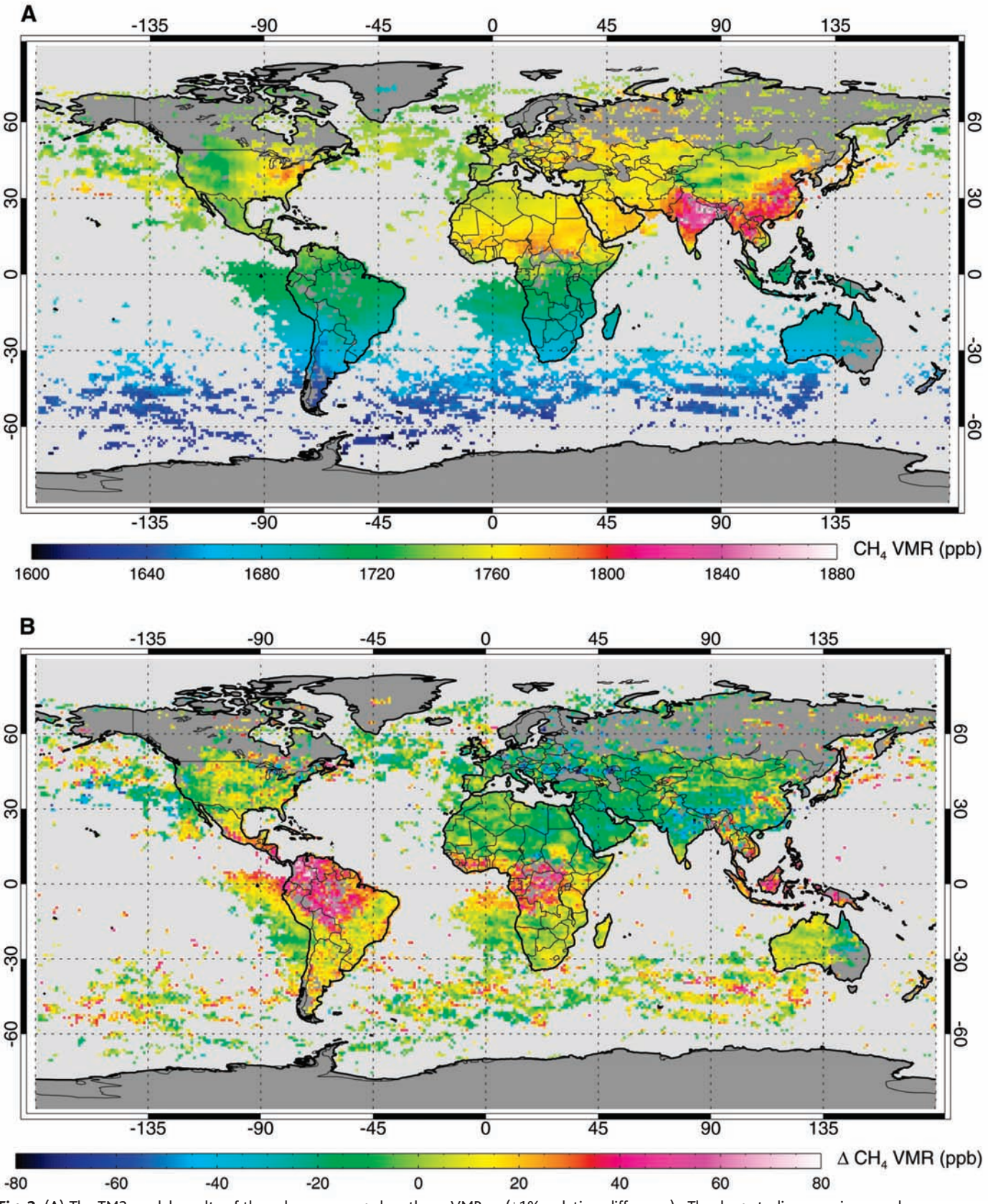

Fig. 3. (**A**) The TM3 model results of the column-averaged methane VMR in ppb for the time period of August through November 2003. Only modeled values that are colocated in space and time with the respective SCIAMACHY measurements are used for the averaging. (**B**) The difference between the SCIAMACHY measurements and the TM3 model results (Δ). The results are displayed in ppb, ranging in most pixels from –20 to 20 ppb (±1% relative difference). The largest discrepancies can be seen over tropical broadleaf evergreen forests in South America, central Africa, and Indonesia. In these areas, measured values are persistently higher than predicted by the model. Prevailing wind directions cause transport of these discrepant concentrations over the oceans (e.g., northwest of South America or west of Africa).

season in the evergreen forests of tropical South America, Africa, and Indonesia are needed to conclude which source type is responsible for the observed discrepancy and to what extent this discrepancy is caused by an underestimated or hitherto unknown methane source. In addition, investigations of satellite data for longer time periods are necessary to estimate the annual methane excess and to constrain the source attribution.

An additional methane source of 30 Tg in 4 months is large but can be accommodated by the uncertainty in the global budget, which is estimated to be 50 to 100 Tg year^{-1} (*1*). Further, surface observations (*24*) are not in disagreement with a large additional tropical source. Methane emitted in the tropics is generally rapidly uplifted by convection, so that the surface stations, which are located in remote ocean sites, are sensitive to these emissions only to a limited extent. Inverse modeling studies based on ground-based measurements (*25*, *26*) have also indicated higher tropical emissions than those estimated from bottom-up inventories. However, this evidence has been rather indirect and uncertain. The present satellite measurements over the tropical land masses are sensitive to the entire atmospheric column, thus directly reflecting enhancement patterns.

Global measurement from space has proven feasible for detection of CH_4 emissions. The satellite's ability to sense sources globally is unique and opens a new window for the analysis of the biogeochemical cycle of methane and anthropogenic impacts. With SCIAMACHY hopefully in operation for several years to come, we should be able to examine the temporal and spatial variations of CH_4 over longer time periods. The integration of these measurements with atmospheric models and precise ground-based observations should greatly reduce uncertainties in the methane source strength, helping to draw a consistent picture of the global methane budget. This will be a high priority for climate research.

References and Notes

1. J. Houghton *et al.*, Eds., *Climate Change 2001: The Scientific Basis* (Cambridge Univ. Press, Cambridge, 2001).
2. J. Lelieveld, P. J. Crutzen, F. J. Dentener, *Tellus* **B50**, 128 (1998).
3. J. G. J. Olivier, J. J. M. Berdowski, in *The Climate System*, J. J. M. Berdowski, R. Guicherit, B. J. Heij, Eds. (A. A. Balkema/Swets and Zeitlinger, Lisse, Netherlands, 2001), pp. 33–78.
4. L. A. Morrissey, G. P. Livingston, *J. Geophys. Res.* **97**, 16661 (1992).
5. B. P. Walter, M. Heimann, *Global Biogeochem. Cycles* **14**, 745 (2000).
6. H. Bovensmann *et al.*, *J. Atmos. Sci.* **56**, 127 (1999).
7. J. P. Burrows *et al.*, *J. Atmos. Sci.* **56**, 151 (1999).
8. T. Wagner *et al.*, *Monitoring of Trace Gas Emissions from Space: Tropospheric Abundances of BrO, NO_2, H_2Co, SO_2, H_2O, O_2 and O_4 as Measured by GOME in Air Pollution X* (WIT Press, Southampton, UK, 2002).
9. U. Platt, *Differential Optical Absorption Spectroscopy (DOAS) in Air Monitoring by Spectroscopic Techniques* (Wiley, New York, 1994).
10. M. Buchwitz, V. Rozanov, J. Burrows, *J. Geophys. Res.* **105**, 15231 (2000).
11. D. M. O'Brien, P. J. Rayner, *J. Geophys. Res.* **107**, 4354 (2002).
12. C. Frankenberg, U. Platt, T. Wagner, *Atmos. Chem. Phys.* **5**, 9 (2005).
13. C. Clerbaux, J. Hadji-Lazaro, S. Turquety, G. Mégie, P. Coheur, *Atmos. Chem. Phys.* **3**, 1495 (2003).
14. S. C. Olsen, J. T. Randerson, *J. Geophys. Res.* **109**, 10.1029/2003JD003968 (2004).
15. F. Dentener, M. van Weele, M. Krol, S. Houweling, P. van Velthoven, *Atmos. Chem. Phys* **3**, 73 (2003).
16. S. Houweling *et al.*, *J. Geophys. Res.* **105**, 8981 (2000).
17. J. A. Van Aardenne, F. J. Dentener, J. G. J. Olivier, C. G. M. Klein Goldewijk, J. Lelieveld, *Global Biogeochem. Cycles* **15**, 909 (2001).
18. K. Gurney *et al.*, *Nature* **415**, 626 (2002).
19. R. S. DeFries, J. R. G. Townshend, *Int. J. Remote Sens.* **15**, 3567 (1994).
20. J. M. Melack *et al.*, *Global Change Biol.* **10**, 530 (2004).
21. A. H. Devol, J. E. Richey, B. R. Forsberg, L. A. Martinelli, *J. Geophys. Res.* **95**, 16417 (1990).
22. M. O. Andreae, P. Merlet, *Global Biogeochem. Cycles* **15**, 955 (2001).
23. M. G. Sanderson, *Global Biogeochem. Cycles* **10**, 543 (1996).
24. Information about the Climate Monitoring and Diagnostics Network (CMDL) can be found online at www.cmdl.noaa.gov/ccgg.
25. R. Hein, P. J. Crutzen, M. Heimann, *Global Biogeochem. Cycles* **11**, 43 (1997).
26. S. Houweling, T. Kaminski, F. J. Dentener, J. Lelieveld, M. Heimann, *J. Geophys. Res.* **104**, 26,137 (1999).

27. Most importantly the authors thank all scientists and engineers involved in the ESA's ENVISAT/SCIAMACHY mission, especially J. P. Burrows and H. Bovensmann from the University of Bremen, as well as the space agencies of Germany [German Aerospace Center (DLR)], Netherlands [Netherlands Agency for Aerospace Programmes (NIVR)], and Belgium [Belgian User Support and Operations Center (BUSOC)]. We also thank R. Washenfelder and G. Toon from Jet Propulsion Laboratory for the updated methane spectral database; S. Sanghavi for proofreading the manuscript; and the Netherlands SCIAMACHY Data Center, in particular A. J. M. Piters and J. van de Vegte from [Royal Netherlands Meteorological Institut (RNMI)], for invaluable assistance in handling the SCIAMACHY data format. We acknowledge the European Commission for supporting the 5th Framework Programme RTD project EVERGREEN (contract number EVG1-CT-2002-00079) and A. P. H. Goede, EVERGREEN project coordinator.

Supporting Online Material

www.sciencemag.org/cgi/content/full/1106644/DC1
Materials and Methods
SOM Text
Figs. S1 to S4
Movie S1

22 October 2004; accepted 9 March 2005
Published online 17 March 2005;
10.1126/science.1106644
Include this information when citing this paper.

A Hydrogen-Rich Early Earth Atmosphere

Feng Tian,[1,2]* Owen B. Toon,[2,3] Alexander A. Pavlov,[2] H. De Sterck[4]

We show that the escape of hydrogen from early Earth's atmosphere likely occurred at rates slower by two orders of magnitude than previously thought. The balance between slow hydrogen escape and volcanic outgassing could have maintained a hydrogen mixing ratio of more than 30%. The production of prebiotic organic compounds in such an atmosphere would have been more efficient than either exogenous delivery or synthesis in hydrothermal systems. The organic soup in the oceans and ponds on early Earth would have been a more favorable place for the origin of life than previously thought.

It is generally believed that the existence of prebiotic organic compounds on early Earth was a necessary step toward the origin of life. Biologically important molecules can be formed efficiently in a highly reducing atmosphere (CH_4- and/or NH_3-rich) (*1*, *2*). They can also be produced efficiently in a weakly reducing atmosphere (*3*–*5*), where one important factor influencing the efficiency of production is the ratio of hydrogen to carbon (*6*–*8*). However, our current understanding of the composition of early Earth's atmosphere suggests it was neither strongly reducing nor hydrogen-rich. The concentrations of CH_4 and NH_3 are thought to have been low (*9*), and the hydrogen mixing ratio is believed to be of the order of 10^{-3} or smaller (*10*). Because it is difficult to produce organics in the atmosphere, two directions of research into the origin of life on Earth have become dominant: synthesis of organic compounds in hydrothermal systems, and exogenous delivery of organic compounds to early Earth (*11*). Here we reexamine the theory of diffusion-limited escape of hydrogen and show that hydrogen escape from early Earth's atmosphere was not as rapid as previously assumed. Hydrodynamic escape should be the dominant mechanism of escape, implying a hydrogen-rich early Earth atmosphere in which organic molecules could be produced efficiently.

The assumption that the escape of hydrogen is limited by diffusion into the hetero-

[1]Astrophysical and Planetary Science Department, [2]Laboratory for Atmospheric and Space Physics, [3]Program in Atmospheric and Oceanic Science, University of Colorado, Boulder, CO 80309, USA. [4]Department of Applied Mathematics, University of Waterloo, Waterloo, Ontario, N2L 3G1, Canada.

*To whom correspondence should be addressed. E-mail: tian@colorado.edu